



# Solid-state NMR study of the kinetics and mechanism of dimethyl ether carbonylation on cesium salt of 12-tungstophosphoric acid modified with Ag, Pt, and Rh



Mikhail V. Luzgin<sup>a,b</sup>, Maxim S. Kazantsev<sup>a</sup>, Galina G. Volkova<sup>a</sup>, Alexander G. Stepanov<sup>a,b,\*</sup>

<sup>a</sup> Borekov Institute of Catalysis, Siberian Branch of Russian Academy of Sciences, Prospekt Akademika Lavrentieva 5, Novosibirsk 630090, Russia

<sup>b</sup> Department of Natural Sciences, Novosibirsk State University, Pirogova Street 2, Novosibirsk 630090, Russia

## ARTICLE INFO

### Article history:

Received 26 February 2013

Revised 27 June 2013

Accepted 18 August 2013

Available online 23 September 2013

### Keywords:

Dimethyl ether

Carbon monoxide

Carbonylation

Mechanism

Kinetics

12-Tungstophosphoric acid

Metal-carbonyls

Solid-state NMR

## ABSTRACT

By using <sup>13</sup>C magic angle spinning (MAS) NMR, the mechanism of dimethyl ether (DME) carbonylation with carbon monoxide has been studied on solid metal-containing acidic cesium salt of 12-tungstophosphoric acid, M/Cs<sub>2</sub>HPW<sub>12</sub>O<sub>40</sub> (M/HPA, M = Ag, Pt, and Rh). The kinetics of the reaction has been monitored with <sup>1</sup>H MAS NMR in situ. Activation of DME occurs on acidic OH groups of M/HPA and gives rise to the surface methoxy groups at 293–473 K. Carbon monoxide forms the surface metal–carbonyl complexes on M/HPA at 293–473 K. The insertion of CO from the carbonyl into the CH<sub>3</sub>–O bond of surface methoxide results in the acetate group attached to the Keggin anion, from which the target product, methyl acetate, is produced under the interaction with dimethyl ether. The reaction rate decreases in the following order: Rh/Cs<sub>2</sub>HPW<sub>12</sub>O<sub>40</sub> ≫ Pt/Cs<sub>2</sub>HPW<sub>12</sub>O<sub>40</sub> > Ag/Cs<sub>2</sub>HPW<sub>12</sub>O<sub>40</sub>, which correlates well with concentration of the reaction intermediates, methoxy groups, and metal–carbonyls. The higher concentration of these intermediates detected on Rh/Cs<sub>2</sub>HPW<sub>12</sub>O<sub>40</sub> is in charge of the higher carbonylation rate on this catalyst with respect to M/HPA (M = Ag, Pt) catalysts.

© 2013 Elsevier Inc. All rights reserved.

## 1. Introduction

Up to date, the carbonylation of methanol mediated by homogeneous iodine Rh and Ir-complexes in the presence of iodide promoter [1–5] represents the main method of the acetic acid production at the industrial level. Taking into account the corrosive properties of iodide compounds, the development of heterogeneous systems that catalyze this reaction in the absence of iodide additives is of great importance. Halide-free carbonylation of methanol and dimethyl ether (DME) has been recently demonstrated to be realized on the acid forms of zeolites (H-MOR, H-BEA, H-ZSM-5) [6–8], solid 12-tungstophosphoric acid (heteropolyacid, HPA), and its cesium salts [9–12]. These results have encouraged studies of the reaction mechanism using kinetic, IR, desorption experiments [7,8], NMR spectroscopy [12–15], as well as theoretical methods [16]. Among all intermediates, suggested for the carbonylation of methanol and DME, only surface methoxy groups have been reliably identified for zeolite-catalyzed reaction [13]. As to the carbonylation on heteropolyacid catalysts is concerned, both the methoxy group and the surface acetate, as well as the processes of their interconversion and transformation into

target products, acetic acid, or methyl acetate, have been monitored [12,15].

We have demonstrated recently that the surface methoxy groups and Rh-carbonyls represent the main intermediates formed from dimethyl ether and carbon monoxide during carbonylation on Rh/Cs<sub>2</sub>HPW<sub>12</sub>O<sub>40</sub> [15]. The insertion of carbon monoxide at the CH<sub>3</sub>–O bond of methoxide occurs at considerably higher temperatures in comparison with that required for the methoxy group formation and further conversion of the acetate fragment generated at this insertion. So, we suppose that the reaction of carbon monoxide insertion represents a rate-determining stage of the carbonylation. The main role of Rh in this catalytic system consists in trapping of carbon monoxide from gaseous phase and its further transfer to the center of dimethyl ether activation [12,15].

In the present paper, we have tried and established the effect of the metal modifier (Ag, Pt, and Rh) loaded on Cs<sub>2</sub>HPW<sub>12</sub>O<sub>40</sub> on the rate of the carbonylation reaction. The <sup>13</sup>C solid-state (MAS, magic angle spinning) NMR and in situ <sup>1</sup>H MAS NMR measurements of the reaction kinetics could be the powerful tools to achieve the research objectives. NMR allows establishment the mechanisms of bifunctional action of such catalysts. The knowledge on the mechanism assists in understanding the principles of the process proceeding and could serve as the base for goal-seeking search of the new carbonylation processes as well as the improvement of existing ones.

\* Corresponding author. Fax: +7 383 330 8056.

E-mail address: [stepanov@catalysis.ru](mailto:stepanov@catalysis.ru) (A.G. Stepanov).

## 2. Experimental

### 2.1. Materials

Cesium salts of 12-tungstophosphoric acid promoted with metals ( $M/Cs_2HPW_{12}O_{40}$ , where  $M = Ag, Pt,$  and  $Rh$ ) were prepared by drop-wise addition of stoichiometric amounts of 0.1 M aqueous solution of cesium nitrate to a mixture of 0.1 M solutions of  $H_3PW_{12}O_{40}$  (HPA) and  $AgNO_3$  or  $H_2PtCl_6$  or  $RhCl_3$ . The resulting suspension was kept under vigorous stirring for 24 h and then was evaporated at 353–373 K to the solid. The synthesized samples of  $M/Cs_2HPW_{12}O_{40}$  contained 1 wt% Ag or Rh and 1.9 wt%, which corresponds to the same atomic concentration of metals, ca.  $100 \mu\text{mol g}^{-1}$ . The chemical analysis confirmed the desired composition specified by the preparation process. X-ray diffraction pattern of the sample revealed the typical body center cubic structure of  $Cs_2HPW_{12}O_{40}$ . The BET surface area of these samples was ca.  $100 \text{ m}^2 \text{ g}^{-1}$ . The concentration of acidic protons in anhydrous samples, measured from  $^1H$  MAS NMR spectra using TMS as internal standard, was ca.  $340 \mu\text{mol g}^{-1}$ , which is in a good accordance with chemical composition.

Dimethyl ether- $^{13}C_2$  (99 atom%  $^{13}C$ ), dimethyl ether (of  $\geq 99.0\%$  purity), carbon monoxide (of  $\geq 99.0\%$  purity), and carbon monoxide- $^{13}C$  (99 atom%  $^{13}C$ ) were purchased from Aldrich Chemical Company Inc. and were used without further purification.

### 2.2. Sample preparation

The samples of Rh and  $Pt/Cs_2HPW_{12}O_{40}$  (~80 mg) were preliminary activated at 473 K in a stream of  $H_2$  for 2 h to reduce partially metal cations species, while  $Ag/Cs_2HPW_{12}O_{40}$  was activated in air atmosphere at 473 K. Further, the samples of  $M/Cs_2HPW_{12}O_{40}$  ( $M = Ag, Pt,$  and  $Rh$ ) were calcined at 523 K for 16 h under vacuum with the residual pressure less than  $10^{-2}$  Pa. Further, the adsorption of DME (ca.  $60\text{--}110 \mu\text{mol g}^{-1}$ ) and carbon monoxide ( $160 \mu\text{mol g}^{-1}$ ) was performed on this sample under vacuum at the temperature of liquid nitrogen. The glass tube of 4 mm o.d. and 10 mm length (microreactor) with the catalyst sample and adsorbates was then sealed off from the vacuum system at the temperature of liquid nitrogen. This axially high symmetric sealed glass tube could be tightly inserted into the 4 mm zirconia rotor for subsequent in situ NMR analysis of the reaction intermediates and products. The reaction was carried out in this sealed glass tube by sample heating directly in NMR probe, if in situ monitoring of the reaction kinetics was performed. In most cases, the reaction was carried out by sample heating outside NMR probe, and further NMR analysis of the reaction intermediates and products formed in the sealed glass microreactor was performed at room temperature.

### 2.3. NMR experiments

$^1H$  and  $^{13}C$  MAS NMR spectra were recorded on the Bruker AVANCE-400 spectrometer (Larmor frequencies of 400.000 and 100.613 MHz, respectively) within the temperature range of 293–493 K for  $^1H$  NMR and at 293 K for  $^{13}C$  NMR. For recording  $^1H$  MAS NMR spectra, Hahn-echo pulse sequence ( $90\text{--}\tau\text{--}180\text{--}\tau\text{--}$ acquisition) was used, where  $\tau$  was equal to the period of rotor spinning, 200  $\mu\text{s}$ . This echo pulse sequence was used to suppress background broad signal from the NMR probe. The following conditions were used for recording the spectra: 4.9  $\mu\text{s}$  length of  $90^\circ$   $^1H$  pulse, the delay time between scans was 3 s. Twenty to forty scans were collected for each  $^1H$  MAS NMR spectrum.

$^{13}C$  MAS NMR spectra with the high power proton decoupling were recorded with or without cross-polarization (CP) denoted be-

low as  $^{13}C$  CP/MAS NMR and  $^{13}C$  MAS NMR. The following conditions were used for recording the spectra with CP: the proton high power decoupling field strength was 11.5 G (4.9  $\mu\text{s}$  length of  $90^\circ$   $^1H$  pulse), contact time was 4 ms at the Hartmann–Hahn matching condition of 50 kHz, and the delay time between scans was 3 s. The single pulse excitation  $^{13}C$  MAS NMR spectra were recorded with  $90^\circ$  flip angle  $^{13}C$  pulses of the 4.9  $\mu\text{s}$  duration and 12 s recycle delay, which satisfies  $10 \times T_1$  condition. High power proton decoupling in these experiments was used only during the acquisition time. A few thousands scans were collected for each  $^{13}C$  CP/MAS NMR and  $^{13}C$  MAS NMR spectrum. The spinning rate was 5–8 kHz.  $^1H$ , and  $^{13}C$  chemical shifts were referenced with respect to TMS as an external standard with accuracy  $\pm 0.5$  ppm. The precision in the determination of the relative line position was 0.1–0.15 ppm. The sample temperature was controlled by the Bruker BVT-2000 variable-temperature unit. The calibration of the temperature inside the rotor was performed with an accuracy of  $\pm 2$  K by using lead nitrate as a  $^{207}Pb$  MAS NMR chemical shift thermometer [17].

## 3. Results and discussion

### 3.1. Activation of dimethyl ether on $M/Cs_2HPW_{12}O_{40}$ ( $M=Ag, Pt,$ and $Rh$ )

In our recent studies, we have shown that the activation of dimethyl ether (DME) occurs on Brønsted acid centers regardless of the presence or the absence of rhodium species on the surface of  $Cs_2HPW_{12}O_{40}$  [15]. So, we suppose that the conversion of DME on the Ag- and Pt-containing heteropolyacids proceeds in a similar way with the formation of the surface methoxy species and a side product – trimethyloxonium cation (TMOC). Fig. 1 shows the  $^{13}C$  CP/MAS NMR spectra recorded for the products formed from the dimethyl ether- $^{13}C_2$  (DME- $^{13}C_2$ ) on the surface of  $M/Cs_2HPW_{12}O_{40}$  ( $M = Ag, Pt,$  and  $Rh$ ).

The signal at 63 ppm with a shoulder at 67 ppm is predominantly observed at room temperature (Fig. 1a). These resonances have earlier attributed to DME adsorbed on different Brønsted acid sites of HPA, e.g., on terminal and bridged oxygen atoms of the Keggin anion [15]. However, the signal at 67 ppm is rather close to that from the protonated dimethyl ether in superacid solution (68 ppm [18]). So, we attribute this resonance to DME protonated by acidic OH group of HPA, whereas that at 63 ppm belongs to the adsorbed ether. The resonance at 80 ppm is the characteristic of trimethyloxonium cation (TMOC) both in solution [18] and on the surface of the solid acid catalysts [12,15,19]. Heating the sample results in appearance of the resonances at 59 and 76 ppm (Fig. 1b). The first signal belongs to the ordinary methoxy group bound to the HPA surface [12,20]. The second one is usually observed only for cesium salts of HPA and is attributed to another type of the surface methoxy group formed on terminal oxygen atom of the Keggin unit and containing cesium cation bound to the oxygen atom (see Scheme 1) [15]. Thus, the conversion of DME on  $M/Cs_2HPW_{12}O_{40}$  occurs according to Scheme 1 producing methoxy groups, protonated ether, and TMOC. Methanol, which should be formed during the DME-to-methoxide conversion (Scheme 1), is transformed further to the methoxy group and water. It should be noted that the concentration of the methoxy group is rather low for both Ag- and  $Pt/Cs_2HPW_{12}O_{40}$  in comparison with that for  $Rh/Cs_2HPW_{12}O_{40}$  catalyst even at the highest temperature of the reaction (see Fig. 1, cf. the intensity of signal at 59 ppm for Ag, Pt, and  $Rh/Cs_2HPW_{12}O_{40}$ ). This may have an essential effect on the carbonylation reaction (*vide infra*).

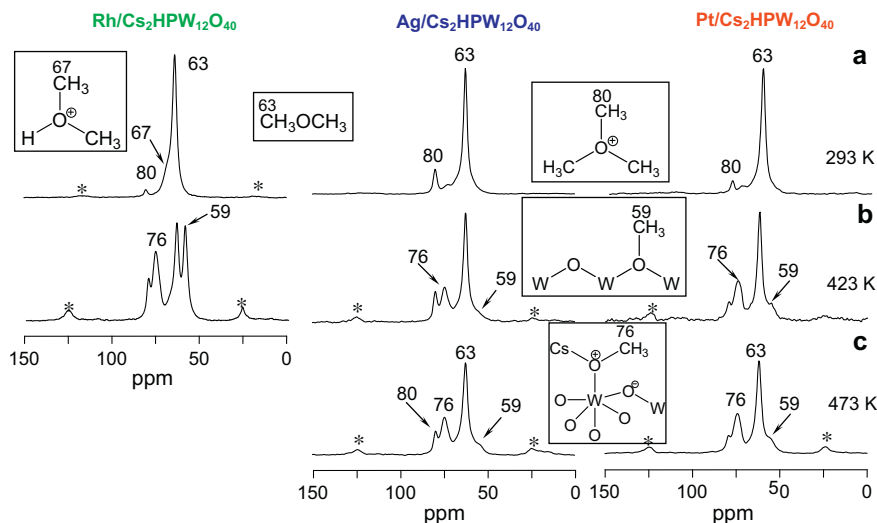
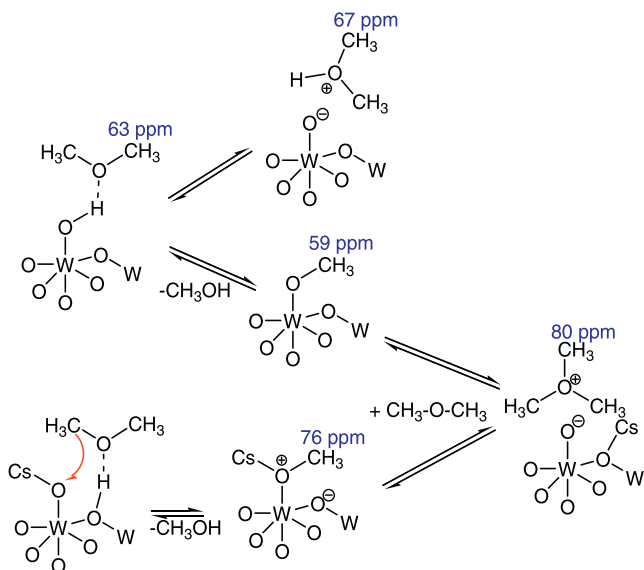


**Fig. 1.**  $^{13}\text{C}$  CP/MAS NMR spectra of the products formed from  $\text{DME-}^{13}\text{C}_2$  on  $\text{M/Cs}_2\text{HPW}_{12}\text{O}_{40}$  ( $\text{M} = \text{Rh}$  (left),  $\text{M} = \text{Ag}$  (middle), and  $\text{M} = \text{Pt}$  (right)) at: (a) 293 K; (b) 423 K; (c) 473 K. Asterisks (\*) denote spinning side-bands.



**Scheme 1.** The common steps of the dimethyl ether activation on  $\text{M/Cs}_2\text{HPW}_{12}\text{O}_{40}$  ( $\text{M} = \text{Ag}$ ,  $\text{Pt}$ , and  $\text{Rh}$ ) at 293–473 K [15,40].

### 3.2. Activation of carbon monoxide on $\text{M/Cs}_2\text{HPW}_{12}\text{O}_{40}$ ( $\text{M} = \text{Ag}$ , $\text{Pt}$ , and $\text{Rh}$ ): the formation of carbonyl complexes

We have previously established that carbon monoxide forms rhodium-carbonyls on the surface of  $\text{Rh/Cs}_2\text{HPW}_{12}\text{O}_{40}$ . This carbonyl serves as the intermediate to transfer CO from gaseous phase to the surface methoxide during the DME carbonylation on this catalyst [15]. So, we have further studied the process of the CO activation on  $\text{Cs}_2\text{HPW}_{12}\text{O}_{40}$  containing Ag or Pt.

Fig. 2 shows  $^{13}\text{C}$  MAS NMR spectra of carbon monoxide- $^{13}\text{C}$  adsorbed on  $\text{M/Cs}_2\text{HPW}_{12}\text{O}_{40}$  ( $\text{M} = \text{Ag}$ ,  $\text{Pt}$ , and  $\text{Rh}$ ). For  $\text{Ag/Cs}_2\text{HPW}_{12}\text{O}_{40}$ , a new signal at 178 ppm, different from that for gaseous  $^{13}\text{C}$  at 183 ppm, is observed already at room temperature (Fig. 2a). Similar signals were found for Ag-carbonyl complexes in solution [21,22]. Hence, carbon monoxide forms Ag-carbonyl complexes on the surface of  $\text{Ag/Cs}_2\text{HPW}_{12}\text{O}_{40}$ .

The adsorption of carbon monoxide on  $\text{Pt/Cs}_2\text{HPW}_{12}\text{O}_{40}$  at room temperature also leads to the formation of surface Pt-carbonyl spe-

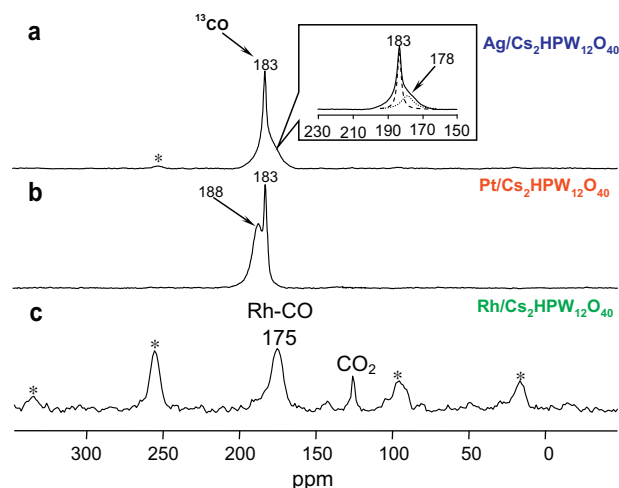


**Fig. 2.**  $^{13}\text{C}$  MAS NMR spectra of the products formed from  $^{13}\text{C}$  at 293–473 K on: (a)  $\text{Ag/Cs}_2\text{HPW}_{12}\text{O}_{40}$ ; (b)  $\text{Pt/Cs}_2\text{HPW}_{12}\text{O}_{40}$ ; (c)  $\text{Rh/Cs}_2\text{HPW}_{12}\text{O}_{40}$ . The spinning rate was 8.0 kHz. Asterisks (\*) denote spinning side-bands.

cies, which signal is observed at 188 ppm [23] (Fig. 2b). Heating the samples at 373–473 K does not cause any change in the spectra of Ag- and Pt-carbonyls. It should be noted in advance that under similar conditions (loaded metal concentration and amount of CO adsorbed), only partial, ca. 60%, conversion of CO into metal-carbonyl is reached in the case of Ag and  $\text{Pt/Cs}_2\text{HPW}_{12}\text{O}_{40}$  at room temperature. At the same time, almost quantitative conversion of CO into Rh-CO species was observed for  $\text{Rh/Cs}_2\text{HPW}_{12}\text{O}_{40}$  [15] (Fig. 2c). Both Ag-CO and Pt-CO surface complexes exist only under the atmosphere of carbon monoxide, and the evacuation of the samples leads to complete disappearance of their signals. So, we were not able to follow the direct interaction of metal-carbonyl with dimethyl ether as in the case of the rhodium catalyst [15]. We have analyzed further the interaction between DME and CO on  $\text{Ag/Cs}_2\text{HPW}_{12}\text{O}_{40}$  and  $\text{Pt/Cs}_2\text{HPW}_{12}\text{O}_{40}$ .

It should be noted that the state of various metals in the metal-carbonyls under study is different. For Rh- and Pt-HPA activated in the hydrogen stream, zero-valence of metal would be expected [24]. However, chemical shift of Rh-CO, 175 ppm, is typical for Rh(I) carbonyl species [25–31]. This implies that Rh(0) is

transformed into Rh(I) in the formed Rh-carbonyl species [32–35]. In contrast to Rh, chemical shift of Pt–CO species, 188 ppm, indicates that the metal exists in the form of highly-dispersed Pt(0) particles [23]. For Ag/HPA, the observed  $^{13}\text{C}$  NMR signal is typical for Ag(I)–CO species [21,22].

### 3.3. Interaction of DME with carbon monoxide on Ag and Pt/ $\text{Cs}_2\text{HPW}_{12}\text{O}_{40}$

Fig. 3 shows the results of the reaction between CO and DME on Ag/ $\text{Cs}_2\text{HPW}_{12}\text{O}_{40}$  and Pt/ $\text{Cs}_2\text{HPW}_{12}\text{O}_{40}$ . The reaction does not proceed up to 423 K, and only small conversion takes place on Pt catalyst (Fig. 3a and b). The reaction starts at 473 K, and methyl acetate is the main product, which is identified by typical signals at 22 ( $\text{CH}_3$ ), 54 ( $\text{CH}_3\text{—O}$ ), and 179 ppm ( $>\text{C=O}$ ) [36,37]. Small intensity resonances at 193 and 22 ppm indicate on the formation of the surface acetate attached to Keggin anion (Keggin acetate) [38]. The formation of the Keggin acetate is the result of the CO insertion into the O– $\text{CH}_3$  bond of surface methoxy group. On Rh/ $\text{Cs}_2\text{HPW}_{12}\text{O}_{40}$ , we observe the direct transformation of rhodium-carbonyl into the  $>\text{C=O}$  moiety of the Keggin acetate, and no free CO exists in gaseous phase. On Ag- and Pt-containing catalysts, metal-carbonyl complexes are in equilibrium with gaseous carbon monoxide (Fig. 1). So, the Keggin acetate can be formed either from the metal-carbonyl or immediately from the gaseous CO on Ag/ $\text{Cs}_2\text{HPW}_{12}\text{O}_{40}$  and Pt/ $\text{Cs}_2\text{HPW}_{12}\text{O}_{40}$  (Scheme 2, stages 1a and 1b). The contribution of stage 1a and 1b will be discussed later (see Section 3.4).

In principle, one cannot exclude the possibility of the intermediate formation of metal-methyl species,  $\text{CO—M—CH}_3$ , especially in the case of rhodium catalyst, via oxidative addition of DME to the metal-carbonyls. This reaction is analogous to oxidative addition of methyl iodide promoter during methanol carbonylation by rhodium complexes in solution [26,39]. Further processes could occur on metal center and include the migratory insertion reaction, affording metal-acetyl complex. Rapid migration of acetyl group from metal center to Brønsted acid site of Rh/ $\text{Cs}_2\text{HPW}_{12}\text{O}_{40}$  could give rise to acetate group attached to the Keggin unit (Keggin acetate). Indeed, such processes are realized on Rh/ $\text{Cs}_2\text{HPW}_{12}\text{O}_{40}$  during the DME carbonylation, but only in the presence of methyl iodide promoter [40]. Methyl iodide forms cis- and trans-Rh-methyl complexes even at room temperature, which are stable in the absence of carbon monoxide and characterized by the resonances at 5 and 14 ppm. In the presence of CO, they readily converts into rhodium-acetyls at its typical position in  $^{13}\text{C}$  NMR spectrum at 49 ( $\text{CH}_3$ -group) and 215 ppm ( $\text{CO}$ -group) [40]. In the presence of Brønsted acid site, Rh-acetyl interacts with OH group to produce Keggin acetate. HI formed at this stage interacts with DME to regenerate reactive  $\text{CH}_3\text{I}$  and, thus, involves the ether into the reaction. However, the situation is quite different in the absence of promoter. For DME itself, the formation of both Rh-methyl species, as well as Rh-acetyls, is never observed on metal-containing HPA used in our study (see Figs. 1,3, Refs. [15,40]). So, this pathway of DME carbonylation on M/ $\text{Cs}_2\text{HPW}_{12}\text{O}_{40}$ , if realizes, gives minor contribution to the process.

Methyl acetate forms from the Keggin acetate under the reaction with DME molecule (Scheme 2, stage 2). Contrary to Ag and

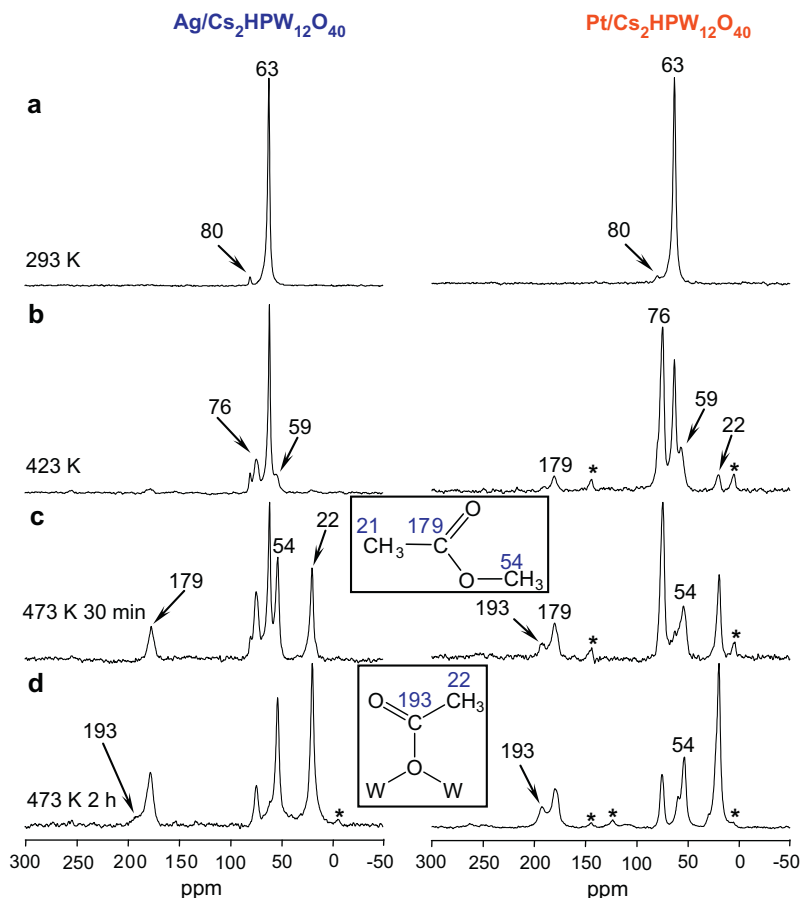
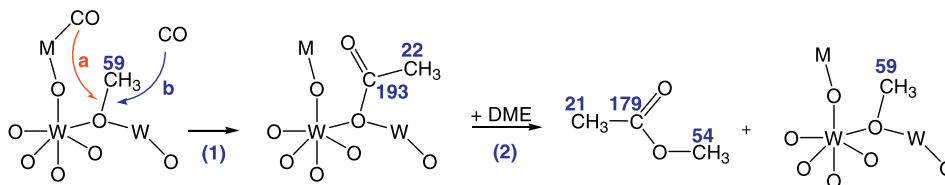


Fig. 3.  $^{13}\text{C}$  CP/MAS NMR spectra of the products formed from DME- $^{13}\text{C}_2$  and  $^{13}\text{CO}$  on Ag/ $\text{Cs}_2\text{HPW}_{12}\text{O}_{40}$  and Pt/ $\text{Cs}_2\text{HPW}_{12}\text{O}_{40}$  at: (a) 293 K; (b) 423 K for 60 min; (c) 473 K for 30 min; (d) 473 K for 2 h. Asterisks (\*) denote spinning side-bands.



**Scheme 2.** The common steps of the dimethyl ether carbonylation on  $M/Cs_2HPW_{12}O_{40}$  ( $M = Ag$  or  $Pt$ ) at 293–473 K [15,40].

$Pt/Cs_2HPW_{12}O_{40}$  catalysts, the Keggin acetate is the main product of the DME carbonylation on  $Rh/Cs_2HPW_{12}O_{40}$  under similar reaction conditions. This is the result of the lower concentration of the unreacted ether, which could interact with Keggin acetate (see Fig. 1). On  $Rh/Cs_2HPW_{12}O_{40}$ , methyl acetate is formed only under the adsorption of additional portion of DME [15].

The carbonylation of DME on  $Ag$  and  $Pt/Cs_2HPW_{12}O_{40}$  proceeds at higher temperature than on  $Rh/Cs_2HPW_{12}O_{40}$  catalyst (*vide infra*, Section 3.4). We have further monitored the kinetics of the DME carbonylation on these three catalysts using  $^1H$  MAS NMR to obtain a detailed information on the reaction rate.

### 3.4. In situ $^1H$ MAS NMR monitoring the kinetics of the DME carbonylation on $M/Cs_2HPW_{12}O_{40}$ ( $M=Ag, Pt, and Rh$ )

Fig. 4 shows the  $^1H$  MAS NMR spectra of DME reacting with carbon monoxide on  $Rh/Cs_2HPW_{12}O_{40}$  in dependence of the reaction time. The decreasing signal at 4.0 ppm is due to the  $CH_3-O$  moiety of the mixture of adsorbed DME, methoxy group, protonated ether, and TMOc [18,41–43]. The increasing resonance at ca. 2.5 ppm arises evidently from the  $CH_3$  groups of both the Keggin acetate and the acetic acid [43]. The signals at 8.8 and 5.0 ppm belong to the acid OH groups of HPA. The first signal is typical for solid heteropolyacids [44–46] and is attributed to strongly acidic or superacidic OH groups [47], which are hydrogen-bonded with neighboring Keggin anions [48]. According to its position in the spectrum, the upfield shifted signal at 5.0 ppm should be assigned to less acidic “free” (like in zeolites) OH groups [49], i.e. without hydrogen bonds. Similar chemical shift of 5.2 ppm was reported for the acid OH groups of  $H_3PW_{12}O_{40}$  dispersed on various supports [45,46]. The signal was attributed to the OH groups of the isolated Keggin anions or small clusters of them, in which no hydrogen-bonding between the Keggin anions exists [45,46].  $Cs_2HPW_{12}O_{40}$  possesses appreciable porosity and surface area, ca.  $100\text{ m}^2\text{ g}^{-1}$ , in contrast to  $5\text{--}10\text{ m}^2\text{ g}^{-1}$  typical for “bulk”  $H_3PW_{12}O_{40}$ . So, cesium salt can indeed contain more protons, which are not hydro-

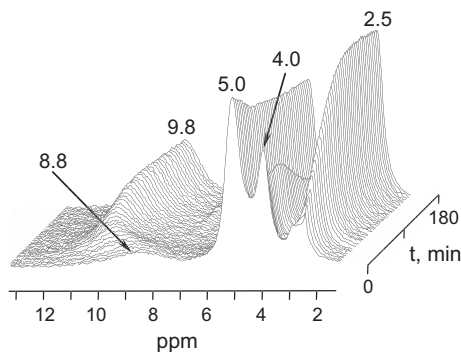


**Fig. 4.** Stack plot of the  $^1H$  MAS NMR spectra at 449 K of DME adsorbed on  $Rh/Cs_2HPW_{12}O_{40}$  and reacting with carbon monoxide. The first spectrum (bottom) was recorded 5 min after the temperature was raised to 449 K and the last spectrum (top) after 180 min of the reaction duration. The time between subsequent spectra recording was 4 min.

gen-bonded with oxygen atoms of adjacent Keggin anions. The intensity of the signal of hydrogen-bonded OH groups increases and shifts to 9.8 ppm during the reaction. This is due to water formed at the DME conversion to the methoxy groups. Water molecules are bounded to the acid OH groups of HPA to form  $H_{2n+1}O_n^+$  cation ( $n = 1, 2$ ) [47], which results to the additional low-field shift of the signal at 8.8 ppm.

Almost quantitative conversion of DME into the carbonylation products occurs (Fig. 4). For obtaining information on the reaction kinetics, we have followed with time the intensity of the signal at 2.5 ppm from the methyl groups. Based on the known initial concentration of DME, the total concentration of the Keggin acetate and acetic acid was calculated.

Fig. 5 shows experimental and simulated kinetics of the DME carbonylation. The experimental points were fitted using a simple function of exponential growth:

$$C_{\text{Acetate+AcOH}} = C_0(1 - e^{-kt}) \quad (1)$$

where  $C_{\text{Acetate+AcOH}}$  is current,  $C_0$  is final total concentration of the surface acetate and acetic acid, and  $k$  is the effective rate constant. Simulation of experimental kinetics offers the effective rate constants  $k$  for the DME carbonylation and its initial rates  $W_{DME}^0 = k \cdot C_0$  at different reaction temperatures (Table 1). Since the reaction is complex and includes the formation of intermediate species, the temperature dependence of initial reaction rate,  $W_{DME}^0$ , was used for the determination of the activation energy. The Arrhenius plot for  $W_{DME}^0$  (Fig. 6) gives the activation energy  $88\text{ kJ mol}^{-1}$ .

Fig. 7 shows the  $^1H$  MAS NMR spectra of DME reacting with carbon monoxide on  $Ag/Cs_2HPW_{12}O_{40}$  in dependence of the reaction time. The signal at 4.0 ppm, which belongs to the  $CH_3-O$  groups of the mixture of adsorbed DME, methoxy group, protonated ether, and TMOc [18,41–43], is decreasing in the course of the reaction. The signal of DME in the gas phase observed at 3.2 ppm in the beginning of reaction disappears in the sequel. The increasing resonances at ca. 2.5 and 4.2 ppm arise from the  $CH_3$  groups in methyl acetate [50]. The signals at 5.4 ppm belong to the acid OH groups of  $Ag/Cs_2HPW_{12}O_{40}$ . We have used the intensity of the signal at 2.5 ppm, and the known initial concentration of DME for obtaining the kinetic curve shown in Fig. 8.

As in the case of  $Rh/Cs_2HPW_{12}O_{40}$  catalyst, we have used the temperature dependence of the initial reaction rate to determine the activation energy (Table 1). The Arrhenius plot for  $W_{DME}^0$  (Fig. 6) affords the activation energy  $85\text{ kJ mol}^{-1}$ , which is similar to that for  $Rh$ -catalyst.

Similar experiments have been carried out for  $Pt/Cs_2HPW_{12}O_{40}$  (spectra and kinetics curves not shown). The results are presented in Table 1 and Fig. 6.

The activation energies for the DME carbonylation proved to be similar for three catalysts under study. However,  $Rh/Cs_2HPW_{12}O_{40}$  is significantly more active than  $Pt/Cs_2HPW_{12}O_{40}$  and  $Ag/Cs_2HPW_{12}O_{40}$ .

To demonstrate the promoting influence of metal on the carbonylation reaction, as well as to accent the role of protons, the reaction rates have been also determined for  $Cs_2HPW_{12}O_{40}$  and  $Rh/Cs_3PW_{12}O_{40}$  samples. The latter contains the same concentration of the

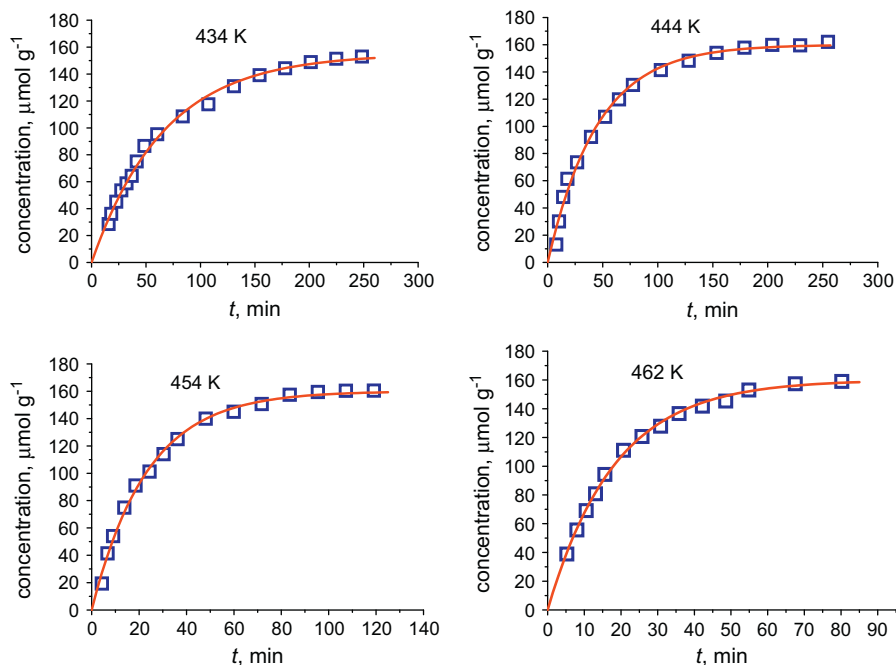


Fig. 5. Experimental and simulated (solid curves) kinetics of DME carbonylation on Rh/Cs<sub>2</sub>HPW<sub>12</sub>O<sub>40</sub>.

Table 1

Initial rates of the DME carbonylation ( $W_{DME}^0$ ,  $\mu\text{mol g}^{-1} \text{min}^{-1}$ ) on M/Cs<sub>2</sub>HPW<sub>12</sub>O<sub>40</sub> catalysts (M = Ag, Pt, and Rh).

T, K	Ag/Cs <sub>2</sub> HPW <sub>12</sub> O <sub>40</sub>	Pt/Cs <sub>2</sub> HPW <sub>12</sub> O <sub>40</sub>	Rh/Cs <sub>2</sub> HPW <sub>12</sub> O <sub>40</sub>	Cs <sub>2</sub> HPW <sub>12</sub> O <sub>40</sub>	Rh/Cs <sub>3</sub> HPW <sub>12</sub> O <sub>40</sub>
434			2.1 ± 0.1		
444			3.6 ± 0.2		
449			4.2 ± 0.3		
454	0.51 ± 0.03	1.0 ± 0.06	6.9 ± 0.4		
462	0.90 ± 0.06	1.38 ± 0.07	8.8 ± 0.4		
473	1.25 ± 0.05	3.2 ± 0.2			
482	2.1 ± 0.2	3.7 ± 0.2		≤1.0	≤0.14

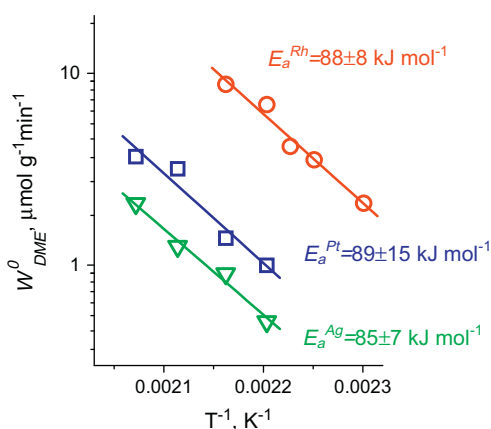


Fig. 6. Arrhenius plots for the initial rate,  $W_{DME}^0$ , of DME carbonylation on: (○) – Rh/Cs<sub>2</sub>HPW<sub>12</sub>O<sub>40</sub>; (□) – Pt/Cs<sub>2</sub>HPW<sub>12</sub>O<sub>40</sub>; (∇) – Ag/Cs<sub>2</sub>HPW<sub>12</sub>O<sub>40</sub>.

metal, but only traces of OH groups. Since the reaction on this samples proceeds very slowly, we can present the results obtained at highest temperature studied (see Table 1). For un-promoted Cs<sub>2</sub>HPW<sub>12</sub>O<sub>40</sub>, the reaction rate is notably lower in comparison with the rates for all M/Cs<sub>2</sub>HPW<sub>12</sub>O<sub>40</sub>. The lowest active catalyst proved to be Rh/Cs<sub>3</sub>HPW<sub>12</sub>O<sub>40</sub>. All these data indicate that the efficiency of metal-containing HPA is determined by the presence of two types

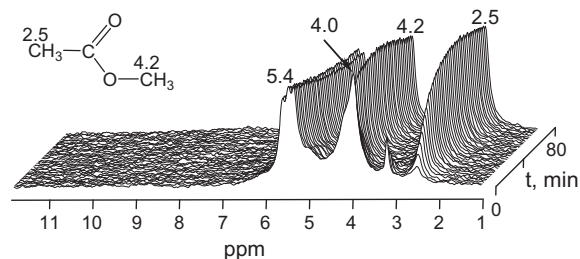


Fig. 7. Stack plot of the <sup>1</sup>H MAS NMR spectra at 482 K of DME adsorbed on Ag/Cs<sub>2</sub>HPW<sub>12</sub>O<sub>40</sub> and reacting with carbon monoxide. The first spectrum (bottom) was recorded 2 min after the temperature was raised to 482 K and the last spectrum (top) after 80 min of the reaction duration. The time between subsequent spectra recording was 1.9 min.

of centers on the catalysts surface: Brønsted acid sites and metal centers. The formation of methoxy group from DME occurs on Brønsted acid sites, while the metal centers provide the delivery of carbon monoxide to the center of DME activation. Thus, stage 1a (Scheme 2) does provide the main pathway of DME carbonylation on metal-containing Cs<sub>2</sub>HPW<sub>12</sub>O<sub>40</sub>. The insertion of CO from M–CO moiety into the CH<sub>3</sub>–O bond of methoxy group appears to be indirect and demands for partial cleavage of M–CO bond due to properties of metal–carbonyls, in which the electronic density on carbon atom is lower in comparison with that on carbon atom of free CO. However, the role of the formation of metal–carbonyl species

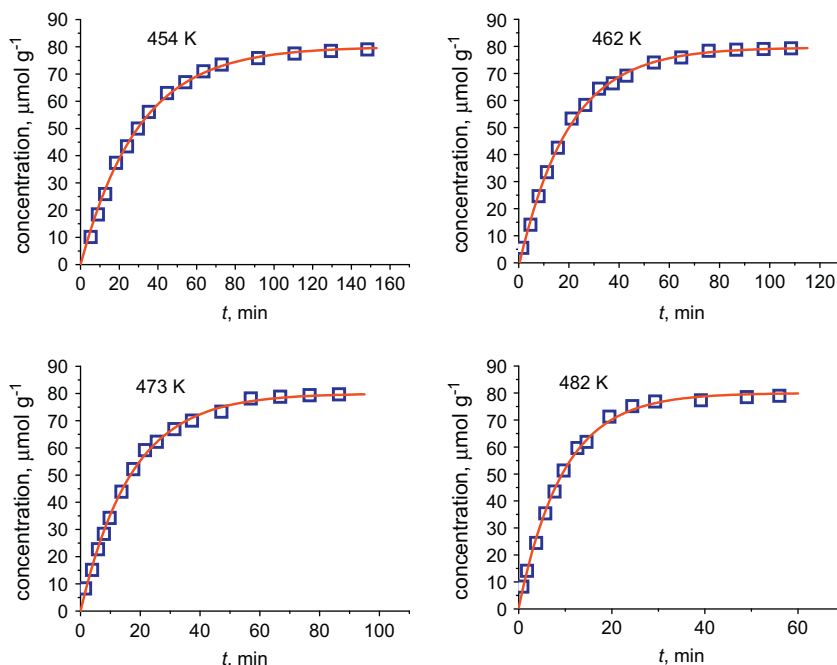


Fig. 8. Experimental and simulated (solid curves) kinetics of DME carbonylation on Ag/Cs<sub>2</sub>HPW<sub>12</sub>O<sub>40</sub>.

consists in increasing lifetime (i.e., increasing the effective concentration) of carbon monoxide in close proximity to surface methoxide, as it was suggested earlier [9]. This favors carbonylation.

The difference in the activity between M/Cs<sub>2</sub>HPW<sub>12</sub>O<sub>40</sub> can be rationalized in terms of relative concentrations of the intermediates formed at the surface of these catalysts. The rate-determining step of the carbonylation reaction on Rh/Cs<sub>2</sub>HPW<sub>12</sub>O<sub>40</sub> is the interaction of Rh-carbonyl with surface methoxide [15]. The situation is similar for Pt- and Ag-containing catalysts. Indeed, the reaction intermediates, the methoxy group and metal-carbonyl, are formed already at 293–423 K, while appreciable interaction between these species and the formation of the carbonylation products occurs at  $\geq 453$  K. The rate of this interaction, as well as the rate of the entire process, is proportional to the concentrations of the intermediate methoxy group and metal-carbonyl:  $W_{DME} \sim [\text{CH}_3\text{—O—W}] \times [\text{M—CO}]$ . Rhodium catalyst provides higher concentration of both methoxy intermediate and carbonyl complex. This can account for the higher reaction rate observed for Rh/Cs<sub>2</sub>HPW<sub>12</sub>O<sub>40</sub>.

As far as methoxy intermediate is concerned, the possible factor determining its concentration can be the nature and the acidity of OH groups of HPA unit. According to <sup>1</sup>H MAS NMR spectra, all the catalysts under study contain a similar concentration of OH groups (ca. 340  $\mu\text{mol g}^{-1}$ ). However, only Rh/Cs<sub>2</sub>HPW<sub>12</sub>O<sub>40</sub> has a significant concentration of strongly acidic OH groups with the signal at 8.8 ppm, whereas Ag- and Pt/Cs<sub>2</sub>HPW<sub>12</sub>O<sub>40</sub> contain presumably less acidic OH groups with the resonances at 5.0–5.4 ppm (cf. bottom spectra of Figs. 4 and 7). Un-promoted HPA, Cs<sub>2</sub>HPW<sub>12</sub>O<sub>40</sub>, revealed similar distribution of the OH groups as Rh/HPA (spectrum not shown) that resulted in similar behavior of both catalysts in the DME activation [12–15]. So, we suppose that the activation of DME on more strong acidic OH groups of Rh/HPA may be the reason for the higher concentration of the methoxy group on this catalyst.

The second point to note is that the concentration of surface carbonyl complexes for Ag and Pt/Cs<sub>2</sub>HPW<sub>12</sub>O<sub>40</sub> is also lower than for Rh-catalyst (see Fig. 2). This fact also contributes to the higher reaction rate achieved on the Rh/Cs<sub>2</sub>HPW<sub>12</sub>O<sub>40</sub>. The reason for the difference in concentrations can be reasonably explained in terms of stability of carbonyl-intermediates. The higher stability of

Rh-carbonyl provides its higher concentration in the reaction with the rhodium catalyst. The possible reason for such order in stability and concentration of metal-carbonyls may be the difference in energy of binding of CO with metal-particles. In this case, the higher binding energy, which could be expected for Rh-catalyst, should increase the activation energy for this catalyst. The second parameter, which could have an influence on the activation energy, is enthalpy of methoxy group formation, as we have already demonstrated for the case of DME carbonylation on H<sub>3</sub>PW<sub>12</sub>O<sub>40</sub> [51]. Lower enthalpy of methoxy group formation for Rh-catalyst can compensate, in principle, the higher binding energy, and we observe nearly the same activation barrier for all samples under study. However, further studies are needed to clarify this issue.

Thus, one should distinguish two principal factors determining the activity of metal-containing heteropolyacids. They reflect the bifunctional character of these catalysts. First, OH groups of strong acidity of HPA structure are needed to provide the DME activation and the formation of the intermediate methoxy groups. The second factor is determined by the choice of metal modifier. The modifier should be capable to perform the capture of carbon monoxide from the gas phase to transfer CO to the center of the DME activation in the form of carbonyl.

#### 4. Conclusions

By using <sup>13</sup>C and <sup>1</sup>H solid-state NMR, the carbonylation of dimethyl ether has been studied on Ag-, Pt-, and Rh-containing acidic cesium salt of 12-tungstophosphoric heteropolyacid.

The mechanism of bifunctional action of these catalysts has been established. Activation of dimethyl ether occurs on Brønsted acid site of the Keggin unit with the formation of the intermediate methoxy groups. Carbon monoxide is transferred to the center of the DME activation through the formation of metal-carbonyls. The insertion of CO from the metal-carbonyl to the CH<sub>3</sub>—O bond of the methoxy group results in acetate fragment attached to the Keggin anion. The later, under the interaction with the DME, leads to the target reaction product, methyl acetate.

The kinetic studies revealed the similar values of the activation energy for all three catalysts, 85–89 kJ mol<sup>-1</sup>, the reaction rate decreasing in the following order: Rh/Cs<sub>2</sub>HPW<sub>12</sub>O<sub>40</sub> ≫ Pt/Cs<sub>2</sub>HPW<sub>12</sub>O<sub>40</sub> > Ag/Cs<sub>2</sub>HPW<sub>12</sub>O<sub>40</sub>. Such a sequence is the result of different concentrations of the reaction intermediates, the methoxy groups, and metal–carbonyls, that are the highest in the case of Rh/Cs<sub>2</sub>HPW<sub>12</sub>O<sub>40</sub>.

## References

- [1] F.E. Paulik, J.F. Roth, *Chem. Commun.* (1968) 1578.
- [2] J.F. Roth, J.H. Craddock, A. Hershman, F.E. Roth, *Chemtech* 1 (1971) 600.
- [3] R.G. Schultz, P.D. Montgomery, *J. Catal.* 13 (1969) 105.
- [4] R.G. Schultz, US Patent 3 717 670, Monsanto Company, 1973.
- [5] M.J. Howard, M.D. Jones, M.S. Roberts, S.A. Taylor, *Catal. Today* 18 (1993) 325.
- [6] B. Ellis, M.J. Howard, R.W. Joyner, K.N. Reddy, M.B. Padley, W.J. Smith, *Stud. Surf. Sci. Catal.* 101 (1996) 771.
- [7] P. Cheung, A. Bhan, G.J. Sunley, E. Iglesia, *Angew. Chem. Int. Edit.* 45 (2006) 1617.
- [8] P. Cheung, A. Bhan, G.J. Sunley, D.J. Law, E. Iglesia, *J. Catal.* 245 (2007) 110.
- [9] R.W. Wegman, *J. Chem. Soc. Chem. Commun.* (1994) 947.
- [10] G.G. Volkova, L.M. Plyasova, A.N. Salanov, G.N. Kustova, T.M. Yurieva, V.A. Likhonobov, *Catal. Lett.* 80 (2002) 175.
- [11] G.G. Volkova, L.M. Plyasova, L.N. Shkuratova, A.A. Budneva, E.A. Paukshtis, M.N. Timofeeva, V.A. Likhonobov, *Stud. Surf. Sci. Catal.* 147 (2004) 403.
- [12] M.V. Luzgin, M.S. Kazantsev, W. Wang, A.G. Stepanov, *J. Phys. Chem. C* 113 (2009) 19639.
- [13] Y. Jiang, M. Hunger, W. Wang, *J. Am. Chem. Soc.* 128 (2006) 11679.
- [14] A. Bhan, A.D. Allian, G.J. Sunley, D.J. Law, E. Iglesia, *J. Am. Chem. Soc.* 129 (2007) 4919.
- [15] M.V. Luzgin, M.S. Kazantsev, G.G. Volkova, W. Wang, A.G. Stepanov, *J. Catal.* 277 (2011) 72.
- [16] M. Boronat, C. Martinez-Sanchez, D. Law, A. Corma, *J. Am. Chem. Soc.* 130 (2008) 16316.
- [17] D.B. Ferguson, J.F. Haw, *Anal. Chem.* 67 (1995) 3342.
- [18] G.A. Olah, H. Doggweiler, J.D. Felberg, S. Fronlich, *J. Org. Chem.* 50 (1985) 4847.
- [19] E.J. Munson, J.F. Haw, *J. Am. Chem. Soc.* 113 (1991) 6303.
- [20] H.L. Zhang, A.M. Zheng, H.G. Yu, S.H. Li, X. Lu, F. Deng, *J. Phys. Chem. C* 112 (2008) 15765.
- [21] P.K. Hurlburt, J.J. Rack, J.S. Luck, S.F. Dec, J.D. Webb, O.P. Anderson, S.H. Strauss, *J. Am. Chem. Soc.* 116 (1994) 10003.
- [22] Y. Souma, H. Kawasaki, *Catal. Today* 36 (1997) 91.
- [23] J.S. Bradley, J.M. Millar, E.W. Hill, S. Behal, *J. Catal.* 129 (1991) 530.
- [24] A.E. Newkirk, D.W. McKee, *J. Catal.* 11 (1968) 370.
- [25] A. Haynes, B.E. Mann, D.J. Gulliver, G.E. Morris, P.M. Maitlis, *J. Am. Chem. Soc.* 113 (1991) 8567.
- [26] A. Haynes, B.E. Mann, G.E. Morris, P.M. Maitlis, *J. Am. Chem. Soc.* 115 (1993) 4093.
- [27] Q. Xu, H. Nakatani, Y. Souma, *J. Org. Chem.* 65 (2000) 1540.
- [28] T.M. Duncan, J.T. Yates, R.W. Vaughan, *J. Chem. Phys.* 71 (1979) 3129.
- [29] T.M. Duncan, J.T. Yates, R.W. Vaughan, *J. Chem. Phys.* 73 (1980) 975.
- [30] T.M. Duncan, T.W. Root, *J. Phys. Chem.* 92 (1988) 4426.
- [31] I.D. Gay, *J. Phys. Chem.* 94 (1990) 1207.
- [32] C.A. Rice, S.D. Worleya, *J. Chem. Phys.* 74 (1981) 6487.
- [33] R.R. Cavanagh, J.T. Yates, *J. Chem. Phys.* 74 (1981) 4150.
- [34] H.F.J. van 't Blik, J.B.A.D. van Zon, T. Huizinga, J.C. Vis, D.C. Koningsberger, R. Prim, *J. Am. Chem. Soc.* 107 (1985) 3139.
- [35] P. Basu, D. Panayotov, J. Yates, J. T., *J. Phys. Chem.* 91 (1987) 3133.
- [36] E. Breitmaier, W. Voelter, <sup>13</sup>C NMR Spectroscopy, Methods and Applications in Organic Chemistry, VCH, Weinheim, 1978.
- [37] D.E. Dorman, B. Bauer, J.D. Roberts, *J. Org. Chem.* 40 (1975) 3729.
- [38] M.V. Luzgin, V.A. Rogov, S.S. Arzumanov, A.V. Toktarev, A.G. Stepanov, V.N. Parmon, *Angew. Chem. Int. Ed.* 47 (2008) 4559.
- [39] A. Haynes, *Top. Organomet. Chem.* (2006) 179.
- [40] M.S. Kazantsev, M.V. Luzgin, G.G. Volkova, A.G. Stepanov, *J. Catal.* 291 (2012) 9.
- [41] G.A. Olah, D.H. O'Brien, *J. Am. Chem. Soc.* 89 (1967) 1725.
- [42] M.J. Lacey, C.G. Macdonald, A. Pross, J.S. Shannon, S. Sternhell, *Aust. J. Chem.* 23 (1970) 1421.
- [43] H.E. Gottlieb, V. Kotlyar, A. Nudelman, *J. Org. Chem.* 62 (1997) 7512.
- [44] Y. Kanda, K.Y. Lee, S. Nakata, S. Asaoka, M. Misono, *Chem. Lett.* (1988) 139.
- [45] V.M. Mastikhin, S.M. Kulikov, A.V. Nosov, I.V. Kozhevnikov, I.L. Mudrakovskii, M.N. Timofeeva, *J. Mol. Catal.* 60 (1990) 65.
- [46] V.M. Mastikhin, V.V. Terskikh, M.N. Timofeeva, O.P. Krivoruchko, *J. Mol. Catal. A* 95 (1995) 135.
- [47] U. Filek, A. Bressel, B. Sulikowski, M. Hunger, *J. Phys. Chem. C* 112 (2008) 19470.
- [48] M. Misono, K. Sakata, Y. Yoneda, W.Y. Lee, Acid-Redox Bifunctional Properties of Heteropoly Compounds of Molybdenum and Tungsten Correlated with Catalytic Activity for Oxidation of Methacrolein, Elsevier, Kodansha (Tokyo), 1980. 1047.
- [49] M. Hunger, *Catal. Rev.-Sci. Eng.* 39 (1997) 345.
- [50] J. McMurry, *Fundamentals of Organic Chemistry*, Cengage Learning, Stamford, 2011.
- [51] M.S. Kazantsev, M.V. Luzgin, A.G. Stepanov, *J. Phys. Chem. C* 117 (2013) 11168.